Comparison between Oxidative Addition and σ-Bond Metathesis as Possible Mechanisms for the Catalytica Methane Activation Process by Platinum(II) Complexes: A Density Functional Theory Study

Thomas M. Gilbert,*[,1] Iordan Hristov, and Tom Ziegler*

Department of Chemistry, University of Calgary, 2500 University Drive NW, Calgary, Alberta, Canada T2N 1N4

Received August 22, 2000

The Catalytica process converts methane to methyl bisulfate in good yield at relatively low temperature in fuming sulfuric acid and may help make methane a useful bulk chemical precursor. We have computationally examined the methane C−H activation step of the process. We find that the most likely catalyst for this step is either (bipyrimidine)$Pt(OSO_3H)^+$ or (bipyrimidine)$PtCl^+$. In the former case C−H activation takes place by σ-bond metathesis, whereas the latter involves C−H activation by an oxidative addition mechanism. It appears that the need to run the reaction at 180−220 °C stems from the fact that methane has to displace either one Cl^- ligand or one HSO_4^- oxygen. Protonation of bipyrimidine by sulfuric acid appears unfavorable, although the resulting highly charged catalysts exhibit lower activation barriers.

Introduction

It has proven difficult to derivatize methane cleanly, specifically, and in high yield. Recent work has focused on sulfonating methane with fuming sulfuric acid. This is motivated by the facts that, one, the presence of the highly oxidized sulfonate group lessens the chance of further oxidation at carbon, two, the ready hydrolysis of the sulfonate group provides the commodity chemical methanol, and three, the SO_2 byproduct readily oxidizes to SO_3, providing a plausible catalytic cycle.

In this regard, the recent report from Periana and coworkers at Catalytica[2] provides great promise. They found that methane reacts with fuming sulfuric acid solvent at modest temperatures (ca. 200 °C) in the presence of (bipyrimidine)$PtCl_2$ to give only methyl bisulfate, with minimal production of byproducts. Yields of >70% of methanol, from hydrolysis of methyl bisulfate, were obtained. Periana et al. proposed a mechanism for this process based on the Shilov C−H activation reactions[3] reported in the 1970s: (1) formation of a 14-electron cationic platinum(II) complex, which reacts with methane to form a platinum(II) methyl compound; (2) oxidation of this material to a platinum(IV) methyl sulfonate compound; and (3) reductive elimination of methyl bisulfate and loss of a bisulfate ligand to regenerate the catalyst (Scheme 1). Labeling studies bear out aspects of this theory, but the nature of the catalyst and the energetics of the system remain poorly explored.

Several theoretical studies have appeared probing this and related processes. Siegbahn and Crabtree examined the Shilov reaction using $(H_2O)_2PtCl_2$ as their catalyst model.[4] They found the C−H bond-breaking step more likely to follow a σ-metathesis path, although an oxidative addition of the C−H bond to the Pt(II) center was energetically competitive. Swang et al., by contrast, find that the lowest energy path for activation of CH_4 by (tmeda)$PtCH_3^+$ involves oxidative addition.[5]

The broadest studies so far come from Hush and coworkers, who examined a variety of plausible intermediates and transition states for all steps of the reaction.[6,7] However, they chose to model the catalyst as *cis*-$(H_3N)PtX_2$, noting that Periana reported that cisplatin [*cis*-diamminedichloroplatinum(II)] catalytically activates methane in sulfuric acid. This lead them to predict transition states for the C−H activation process involving loss of coordinated ammonia. Such dissociations are extremely unlikely for the bidentate, π-accepting bipyrimidine ligand system. Indeed, cisplatin's catalytic abilities decayed rapidly under Periana's reaction conditions, while the bipyrimidine catalyst proved far more active and stable.

The density functional theory study below examines bipyrimidine-substituted platinum catalysts explicitly, modeling the activation of the C−H bond in CH_4 by the tricoordinated complexes (bipyrimidine)PtX^+ (X = Cl^- or HSO_4^-) as well as the diprotonated species (bipyrimidineH_2)$Pt(X)^{3+}$ (X = Cl^- or HSO_4^-). We use the data to

(1) On sabbatical from Department of Chemistry and Biochemistry, Northern Illinois University, DeKalb, IL 60115. Address correspondence to this author at this address, or e-mail: tgilbert@marilyn.chem.niu.edu.

(2) Periana, R. A.; Taube, D. J.; Gamble, S.; Taube H.; Satoh T.; Fujii, H. *Science* **1998**, *280*, 560−564

(3) Shilov, A. E. *Activation of Saturated Hydrocarbons by Transition Metal Complexes*; D. Riedel: Dordrecht, The Netherlands, 1984.

(4) Siegbahn, P. E. M.; Crabtree, R. H. *J. Am. Chem. Soc.* **1996**, *118*, 4442−4450.

(5) Heiberg, H.; Swang, O.; Ryan, O. B.; Gropen, O. *J. Phys. Chem. A* **1999**, *103*, 10004−10008.

(6) Mylvaganam, K.; Bacskay, G. B.; Hush, N. S. *J. Am. Chem. Soc.* **1999**, *121*, 4633−4639.

(7) Mylvaganam, K.; Bacskay, G. B.; Hush, N. S. *J. Am. Chem. Soc.* **2000**, *122*, 2041−2052.

10.1021/om0007264 CCC: $20.00
Publication on Web 02/07/2001

Scheme 1

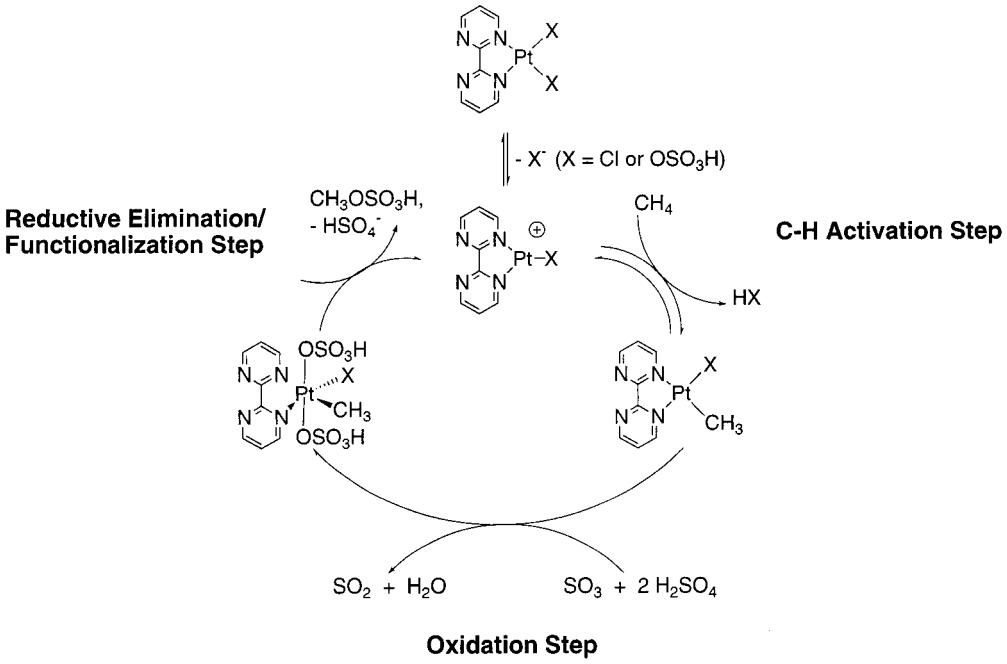

Scheme 2

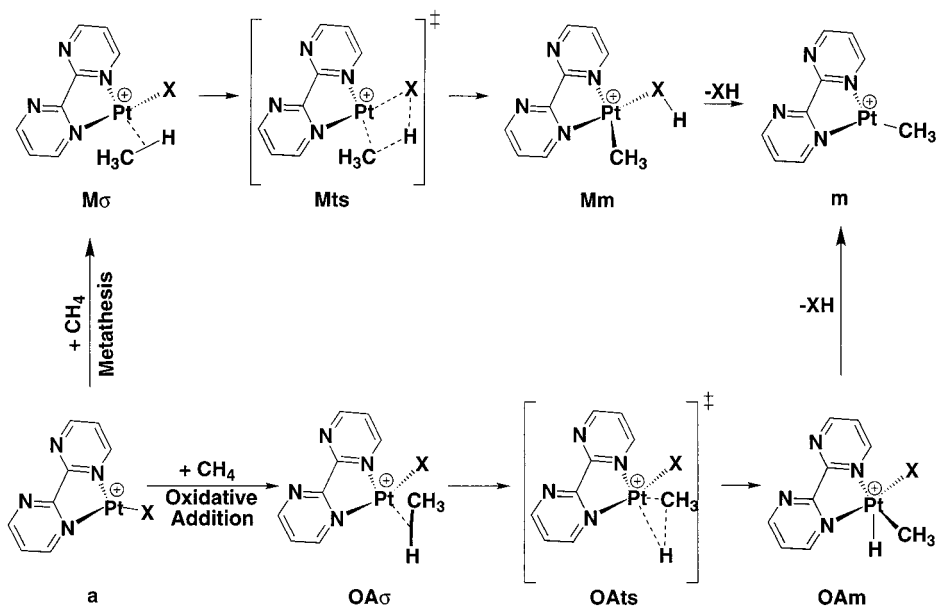

gauge the influence of the peripheral X ligand and of protonating the bipyrimidine ligand on the C−H activation process, emphasizing how different ligand environments influence the relative preference for oxidative addition or σ-bond metathesis as the prevailing mechanism (Scheme 2).

Computational Details

All DFT calculations were carried out using the Amsterdam Density Functional (ADF 2.3.3) program[8] developed by Baerends et al.[9] and vectorized by Ravenek.[10] The numerical integration scheme applied for the calculations was developed by te Velde et al.;[11] the geometry optimization procedure was based on the method of Versluis and Ziegler.[12] Geometry optimizations were carried out and energy differences determined using the local density approximation of Vosko, Wilk, and Nusair (LDA VWN)[13] augmented with the nonlocal gradient correction PW91 from Perdew and Wang.[14] Relativistic corrections were added using a scalar-relativistic Pauli Hamiltonian.[15] The electronic configurations of the molecular

(8) Amsterdam Density Functional program, Division of Theoretical Chemistry, Vrije Universiteit, De Boelelaan 1083, 1081 HV Amsterdam, The Netherlands; http://www.scm.com.

(9) (a) Baerends, E. J.; Ellis, D. E.; Ros, P. *Chem. Phys.* **1973**, *2*, 41−51. (b) Baerends, E. J.; Ros, P. *Chem. Phys.* **1973**, *2*, 52−59.

(10) Ravenek, W. In *Algorithms and Applications on Vector and Parallel Computers*; te Riele, H. J. J., Dekker, T. J., van de Horst, H. A., Eds.; Elsevier: Amsterdam, The Netherlands, 1987.

(11) (a) te Velde, G.; Baerends, E. J. *J. Comput. Chem.* **1992**, *99*, 84−98. (b) Boerrigter, P. M.; te Velde, G.; Baerends, E. J. *Int. J. Quantum Chem.* **1988**, *33*, 87−113.

(12) Versluis, L.; Ziegler, T. *J. Chem. Phys.* **1988**, *88*, 322−328.

(13) Vosko, S. H.; Wilk, L.; Nusair, M. *Can. J. Phys.* **1980**, *58*, 1200−1211.

(14) Perdew, J. P.; Chevary, J. A.; Vosko, S. H.; Jackson, K. A.; Pederson, M. R.; Singh, D. J.; Fiolhais, C. *Phys. Rev. B* **1992**, *46*, 6671−6687.

systems were described by a triple-ζ basis set for all atoms. Non-hydrogen atoms were assigned a relativistic frozen core potential, treating as core the shells up to and including 4f for Pt, 2p for Cl and S, and 1s for N, O, and C. A set of auxiliary s, p, d, and f functions, centered on all nuclei, was used to fit the molecular density and represent Coulomb and exchange potentials accurately in each SCF cycle. Transition states were located from a linear transit scan. The reaction coordinate was kept fixed while optimizing all other degrees of freedom. The value of the constrained parameter was varied until the force acting on it proved smaller than 0.0015 au. That the minimum located corresponded to a transition state was confirmed by demonstrating that changing the reaction coordinate in one direction gave a force of opposite sign of that resulting from changing the reaction coordinate in the opposite direction. This procedure gives only an upper bound for the activation energy. However, from previous work in this area[16] we know it gives results within fractions of kcal mol^{-1} of those from transition state search algorithms and so is sufficiently accurate for our needs. Because of the number of molecules investigated and the computational effort connected with the calculation of second derivatives of the energy with respect to the nuclei positions (the ADF program does this through laborious numerical integration), we refrained from calculating Hessian matrices to confirm that the transition state structures determined exhibited the required imaginary frequencies.

As the calculated structures typically exhibit expected bond distances and angles, particularly for the spectator ligands, only notable parameters are given in the text below. More detailed structural data are available as Supporting Information. The energy differences in solution were derived from gas phase energies and structures by estimating solvation energies using the Conductor-like Screening Model (COSMO),[17] which was recently implemented within the ADF program.[18] The solvation calculations were performed with a dielectric constant of 100 for sulfuric acid. The radii (in Å) used for the atoms were as follows: hydrogen 1.16, sulfur 1.7, carbon 2.3, oxygen 1.3, chlorine 1.8, nitrogen 1.4, and platinum 1.387. These values were obtained by optimization using least-squares fitting to experimental solvation energies.

Results and Discussion

A graph comparing the relative energies of the species (**na**, **nOAs**, **nOAts**, and **nOAm**) involved in the oxidative addition processes appears in Figure 1. The integer *n* in the labels of Figure 1 refers to derivatives of (bipyrimidine)$PtCl^+$ ($n = 1$), (bipyrimidineH_2)$PtCl^{3+}$ ($n = 2$), (bipyrimidine)$Pt(OSO_3H)^+$ ($n = 3$), and (bipyrimidineH_2)$Pt(OSO_3H)^{3+}$ ($n = 4$), respectively. Figures2 and 3 contain similar diagrams for the metathesis reactions for the cases of $n = 1$, 2 and $n = 3$, 4, respectively. Full details about the optimized structures can be found in the Supporting Information; however, the basic features can be gleaned from the figures. The relative energies (kcal mol^{-1}) in the gas phase are shown in parentheses, and the corresponding solution phase values appear without parentheses.

(Bipyrimidine)$PtCl^+$, 1a, and (BipyrimidineH_2)-$PtCl^{3+}$, 2a. The computational model predicts a preference for oxidative addition over metathesis when catalyst **1a** reacts with CH_4. In the first step in each case, methane coordinates to the metal through a C−H σ-bond, lowering the energy of the systems by −14.5 kcal mol^{-1} (**1OAσ**) and −9.9 kcal mol^{-1} (**1Mσ**), respectively. Comparison of the structures of the resulting **1OAσ** and **1Mσ** compounds shows how similar the two are; they differ most in the angle between the Pt−C−H bond plane and the Pt−N_2−Cl plane (90° for **1OAσ**, 0° for **1Mσ**). The Pt−C and Pt−H distances are nearly identical, being 2.349 and 1.746 Å for the former and 2.354 and 1.736 Å for the latter. For the metathesis process, the σ-bound minimum lies early in the bond-breaking process, as the coordinated CH bond is only slightly stretched to 1.147 Å. For the oxidative addition process, the σ-complex lies slightly later in the bond-breaking process, with a coordinated CH bond length of 1.165 Å.

In both cases, the C−H bond then stretches substantially until the transition state is attained, with an energy barrier of 10.0 kcal mol^{-1} (**1OAts**) and 17.3 kcal mol^{-1} (**1Mts**), respectively. At the oxidative addition transition state **1OAts**, the C−H bond has essentially broken (2.122 Å) and the Pt−C (2.053 Å) and Pt−H (1.512 Å) bonds have fully formed. Its structure predicts

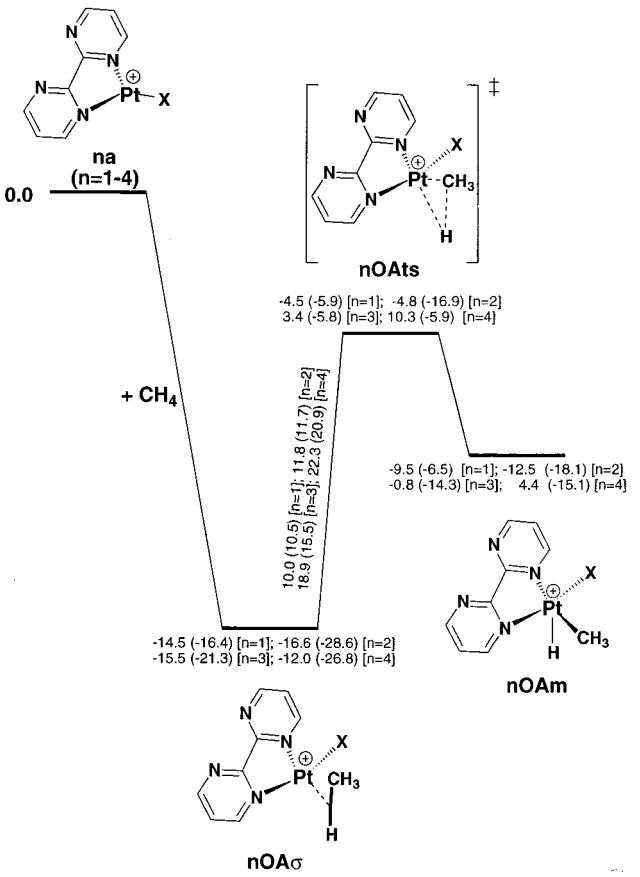

Figure 1. Graph comparing the relative energies of the species (**na**, **nOAσ**, **nOAts**, and **nOAm**) involved in the oxidative addition processes. The integer *n* in the labels refers to derivatives of (bipyrimidine)$PtCl^+$ ($n = 1$), (bipyrimidineH_2)$PtCl^{3+}$ ($n = 2$), (bipyrimidine)$Pt(OSO_3H)^+$ ($n = 3$), and (bipyrimidineH_2)$Pt(OSO_3H)^{3+}$ ($n = 4$), respectively. The relative energies (kcal mol^{-1}) in the gas phase are shown in parentheses and the corresponding numbers in solution without parentheses. Energies are relative to **na**.

(15) Snijders, J. G.; Baerends, E. J.; Ros, P. *Mol. Phys.* **1979**, *38*, 1909−1929.
(16) (a) Margl, P. M.; Deng, L.; Ziegler, T. *Organometallics* **1998**, *17*, 933−946. (b) Margl, P. M.; Deng, L.; Ziegler, T. *J. Am. Chem. Soc.* **1998**, *120*, 5517−5525. (b) Margl, P. M.; Deng, L.; Ziegler, T. *J. Am. Chem. Soc.* **1999**, *121*, 154−162.
(17) Klamt, A.; Schuurmann, G. *J. Chem. Soc., Perkin Trans.* **1993**, *2*, 799−805.
(18) Pye, C. C.; Ziegler, T. *Theor. Chem. Acc.* **1999**, *101*, 396−408.

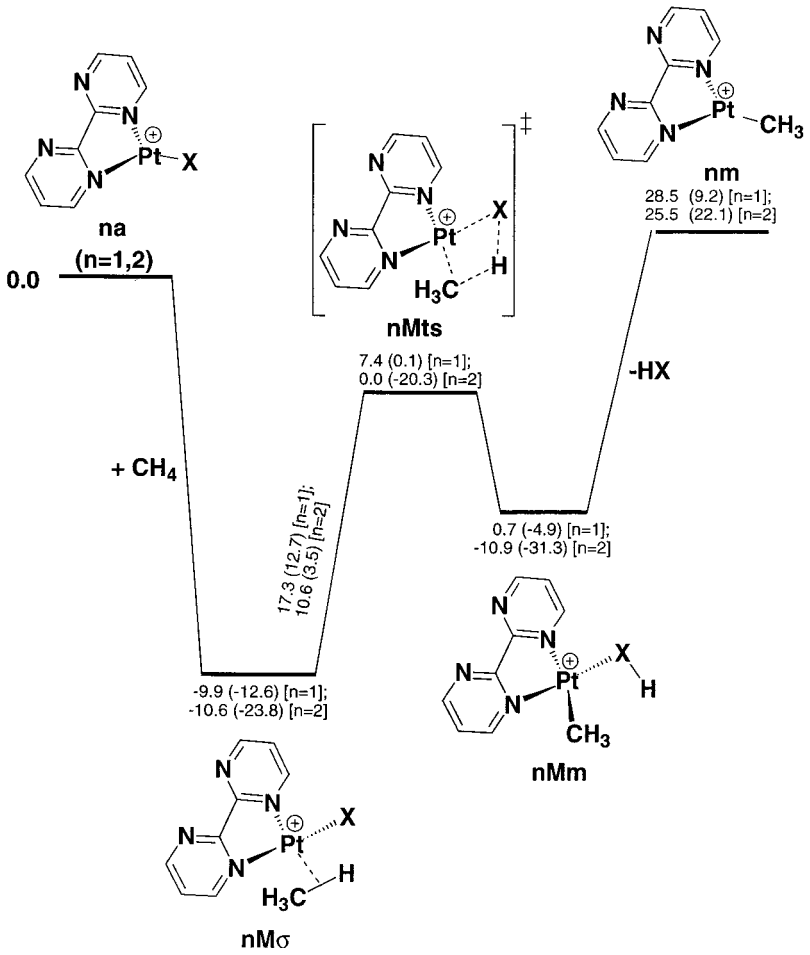

Figure 2. Graph comparing the relative energies of the species (**na**, **nMσ**, **nMts**, **nMm**, and **nm**) involved in the metathesis processes of the platinum chloride catalysts. The integer *n* in the labels refers to derivatives of (bipyrimidine)$PtCl^+$ (n = 1) and (bipyrimidineH_2)$PtCl^{3+}$ (n = 2), respectively. The relative energies (kcal mol^{-1}) in the gas phase are shown in parentheses and the corresponding numbers in solution without parentheses. Energies are relative to **na**.

that the transition state will lead to the H-axial isomer **1OAm**, rather than a C-axial isomer, as the hydrogen atom lies farther above the Pt−N−N−Cl plane than the carbon lies below it. The metathesis transition state **1Mts** is more complex, as the platinum atom interacts weakly (Pt−H distance = 2.122 Å) with the hydrogen atom to "pass it along" to the chlorine atom (H−Cl distance = 1.472 Å). Despite these interactions, and though the Pt−C bond is nearly fully formed (Pt−C distance = 2.066 Å), a CH interaction remains (CH distance = 1.575 Å).

Passage through the transition states affords the methyl complexes **1OAm** (−9.5 kcal mol^{-1}) and **1Mm** (0.7 kcal mol^{-1}). Thus, the oxidative addition product **1OAm** is favored both kinetically and thermodynamically over the metathesis product **1Mm**. Overall, the key C−H activation steps **1OAσ** → **1OAm** (+5.0 kcal mol^{-1}) and **1Mσ** → **1Mm** (+10.6 kcal mol^{-1}) are both endothermic. However, the metathesis step is the least favorable.

That the Periana reaction occurs in concentrated sulfuric acid opens up the possibility that the peripheral nitrogen atoms of the bipyrimidine ligand are protonated in the catalyst.[19] This would increase the positive charge at platinum and benefit the σ-bond metathesis mechanism[20] relative to the oxidative addition pathway by favoring the electrophilic attack of the metal center on the C−H bond in the former. We estimated the degree of protonation by calculating the enthalpy for the single and double protonation processes, using the results from this study:

$$\text{(bipyrimidine)}PtCl^+ + H_2SO_4 \rightarrow \text{(Hbipyrimidine)}PtCl^{2+} + HSO_4^- \quad (1)$$

$$\text{(bipyrimidine)}PtCl^+ + 2H_2SO_4 \rightarrow \text{(}H_2\text{bipyrimidine)}PtCl^{3+} + 2HSO_4^- \quad (2)$$

We find both to be endothermic with reaction energies of 6.9 and 34.2 kcal mol^{-1}, respectively. These estimates suggest either that the peripheral bipyrimidine nitrogen atoms are not protonated in the Catalytica catalyst or that if they are, then counterions probably coordinate to the metal as well. The overall charge on the catalyst remains small.

However, in case the computational model does not accurately describe the molecular behavior in hot, fuming, highly protic sulfuric acid, we explored the methane activation reaction by examining the mecha-

(19) Stahl, S. S.; Labinger, J. A.; Bercaw, J. E. *Angew. Chem., Int. Ed.* **1998**, *37*, 2180−2192.

(20) Spessard, G. O.; Miessler, G. L. *Organometallic Chemistry*; Prentice Hall: Upper Saddle River, NJ, 1997; Sections 7-2 and 10-7.

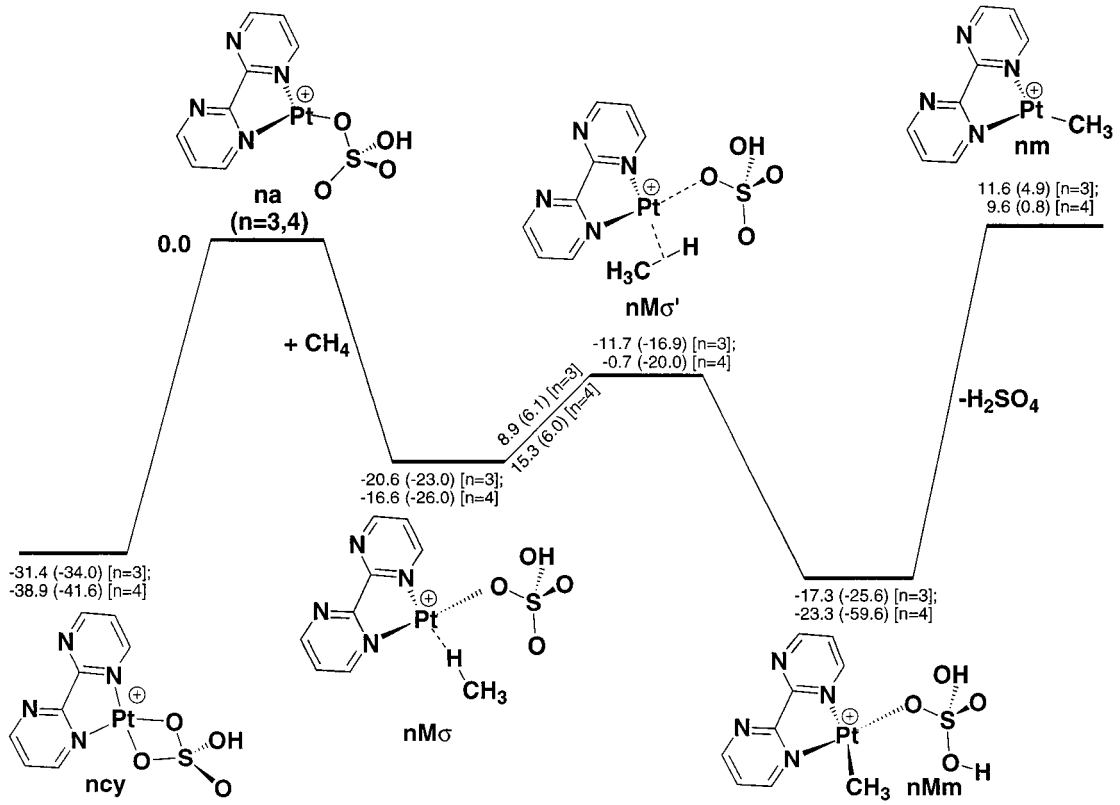

Figure 3. Graph comparing the relative energies of the species (**ncy**, **na**, **nM*σ***, **nM*σ′***, **nMm**, and **nm**) involved in the metathesis processes of the platinum bisulfate catalysts. The integer *n* in the labels refers to derivatives of (bipyrimidine)-$Pt(OSO_3H)^+$ (*n* = 3) and (bipyrimidineH_2)$Pt(OSO_3H)^{3+}$ (*n* = 4), respectively. The relative energies (kcal mol^{-1}) in the gas phase are shown in parentheses and the corresponding numbers in solution without parentheses. Energies are relative to **na**.

nistic steps above for tricationic **2a**. This starting point was chosen over one containing coordinated counterions for computational simplicity and for ease of comparison with the **1a** → **1m** processes. Molecules containing coordinated counterions will be described in future publications.[21]

The model starting with **2a** again exhibits a preference for oxidative addition over metathesis, but a substantially reduced one. The larger positive charge increases the Lewis acidity of the platinum center, resulting in a moderately larger exothermicity for the formation of the *σ*-bond complexes **2OA*σ*** (−16.6 kcal mol^{-1}) and **2M*σ*** (−10.6 kcal mol^{-1}) compared to **1OA*σ*** (−14.5 kcal mol^{-1}) and **1M*σ*** (−9.9 kcal mol^{-1}). The transition state **2OAts** for the oxidative addition at −4.8 kcal mol^{-1} is still of lower energy than the transition state **2Mts** at 0.0 kcal mol^{-1}. However, the energy difference between **nOAts** and **nMts** has been reduced from 11.9 kcal mol^{-1} for *n* = 1 to 4.8 kcal mol^{-1} for *n* = 2. Further, the internal barrier for metathesis of 10.6 kcal mol^{-1} is slightly lower than the barrier of 11.8 kcal mol^{-1} associated with the oxidative addition process.

The oxidative addition product **2OA** (−12.5 kcal mol^{-1}) is calculated to be more stable than the metathesis product **2Mm** (−10.9 kcal mol^{-1}). However, the energy difference between **nOA** and **nMm** decreases from 10.2 kcal mol^{-1} for *n* = 1 to 1.6 kcal mol^{-1} for *n* = 2. Further, the metathesis process **2M*σ*** → **2Mm** is exothermic by 0.3 kcal mol^{-1}, while the oxidative addition process **2OA*σ*** → **2OA** is endothermic by 4.1 kcal mol^{-1}. As expected, protonating the bipyrimidine ligand enhances the metathesis pathway compared to the oxidative addition pathway.

Also shown in Figures 1 and 2 (in parentheses) are the relative energies in the gas phase. The values show a general trend of stabilization for all species when solvation is not included. Furthermore, the intermediates and transition states along the pathways (**nMs**, **nOAs**, etc.) are stabilized considerably relative to **na** and methane. The metathesis process gains more from this stabilization than does the oxidative addition reaction, becoming the favored pathway for **2a** → **2m**. As above, this arises from the tripositive charge on **2a**.

(Bipyrimidine)$PtOSO_3H^+$, 3a, and (BipyrimidineH_2)$PtOSO_3H^{3+}$, 4a. Another possible consequence of performing the methane activation reaction in fuming sulfuric acid is the replacement of the chloride ligands with bisulfate ligands. We explored the benefits of this substitution by examining the reaction pathways available to the bisulfate-substituted species (bipyrimidine)-$PtOSO_3H^+$, **3a**, and (bipyrimidineH_2)$PtOSO_3H^{3+}$, **4a**. Figure 1 gives the relative energies for the oxidative addition process starting with (bipyrimidine)$PtOSO_3H^+$ (*n* = 3) and (bipyrimidineH_2)$PtOSO_3H^{3+}$ (*n* = 4), respectively. A similar diagram for the metathesis process appears in Figure 3.

We find, as did Hush and co-workers,[6] that the bisulfate ligand forms bidentate complexes **3cy** and **4cy**, which are more stable than **3a**/**4a** by 31.4 and 38.9 kcal

(21) Hristov, I.; Ziegler, T., work in progress.

mol^{-1}, respectively (for clarity, these are shown only in Figure 3). These relatively high energies required to dissociate one oxygen atom provide a reason that one must conduct the reaction at 180−200 °C, assuming that **3a** or **4a** is the catalyst for the methane activation process (see below). Once the dissociation occurs, no later C−H activation step requires a comparable energy input.

The oxidative addition pathway for the bisulfate complex **3a** (Figure 1) resembles that of the chloride analogue. The only notable distinction is that the transition state **3OAts** exhibits a CH bond length of 1.729 Å and thus lies earlier along the path than for the chloride system. The process **3OA*σ* → 3OAm** is calculated to be more endothermic (by 9.7 kcal mol^{-1}) than the analogous reaction **1OA*σ* → 1OAm**. We attribute this to the fact that the metal center is less electron rich with OSO_3H^- as the ligand and thus less likely to undergo oxidative addition. This is also reflected in the activation barrier, which increases from 10.0 kcal mol^{-1} (**1OA*σ* →1OAm**) to 18.9 kcal mol^{-1} (**3OA*σ* → 3OAm**).

The metathesis pathway, however, differs starkly from that of the chloride (Figure 3 vs Figure 2). The *σ*-complex **3M*σ*** exhibits a short Pt−H distance (1.514 Å) and a linear (180°) Pt−H−C angle; no Pt−C interaction exists. For the metathesis reaction to succeed, the *σ*-complex **3M*σ*** must rearrange to another *σ*-adduct **3M*σ′***, where the C−H bond coordinates to Pt (Figure 3). From **3M*σ′***, analogy with the chloride system dictates transfer of the H atom to the Pt-bound bisulfate O atom (forming **3Mm′**; see below). However, a lower energy path is available, wherein the activated H atom of **3M*σ′*** transfers directly from to a *peripheral* bisulfate O atom, forming the stable product **3Mm**. We find no barrier for this remarkable step by linear transit studies beginning with both **3M*σ′*** and **3Mm**. Evidently the proximity and basicity of the peripheral oxygen atoms make transfer of the carbon-bound hydrogen to them easy. We note no distinguishing bond distances or angles between **3M*σ′*** and the analogous **1M*σ***; in **3M*σ′***, the Pt−C distance is 2.370 Å, the Pt−H distance is 1.676 Å, and the C−H distance is 1.138 Å. The transferring hydrogen atom is closer to the Pt-bound oxygen atom (2.178 Å) than to any peripheral one, but a modest rotation of the SO_3H moiety brings a peripheral oxygen to 2.155 Å from the hydrogen. The linear transit studies indicate the utilization of this rotation prior to hydrogen transfer. Because of the stability of **3Mm**, the process **3M*σ* → 3Mm** is modestly endothermic by 3.3 kcal mol^{-1} and energetically more favorable than the corresponding oxidative addition process **3OA*σ* → 3OAm**, which has an endothermicity of 14.7 kcal mol^{-1}. Thus, the replacement of Cl^- in **1a** by OSO_3H^- in **3a** shifts the preference for the reaction between **na** and CH_4 from oxidative addition ($n = 1$) to metathesis ($n = 3$) as the charge on the metal center is increased. We finally note that the isomer (**3Mm′**) of **3Mm** in which H_2SO_4 binds to platinum through a hydroxy oxygen is less stable by 5.6 kcal mol^{-1}.

As above for the chloride-containing **1a**, we estimated the degree of protonation by calculating the enthalpy for the single and double protonation processes for **3a**, using the results from this study:

$$(\text{bipyrimidine})PtOSO_3H^+ + H_2SO_4 \rightarrow (\text{Hbipyrimidine})PtOSO_3H^{2+} + HSO_4^- \quad (3)$$

$$(\text{bipyrimidine})PtOSO_3H^+ + 2H_2SO_4 \rightarrow (H_2\text{bipyrimidine})PtOSO_3H^{3+} + 2HSO_4^- \quad (4)$$

We find both to be endothermic with reaction energies of 3.6 and 25.6 kcal mol^{-1}, respectively. Though these values are somewhat lower than those for the analogous chlorides, they still suggest that the overall charge on the catalyst remains small.

As above, however, we felt it worthy to examine the mechanistic steps for tricationic **4a**. As in the chloride case, the additional positive charge on catalyst **4a** engendered by protonating the bipyrimidine ring has a modest effect on the oxidative addition pathway (Figure 1). The key part of the pathway, **4OA*σ* → 4OAm**, is endothermic by 16.4 kcal mol^{-1}, an increase of only 1.8 kcal mol^{-1} compared to **3OA*σ* → 3OAm.** On the other hand, changing the ligand from Cl^- (**2OA*σ* → 2OAm**) to OSO_3H^- (**4OA*σ* → 4OAm**) increases the endothermicity by 12.3 kcal mol^{-1} and the barrier by 10.5 kcal mol^{-1}. As above, this substitution makes the metal center less electron-rich and consequently the oxidative addition more difficult.

By contrast, double protonation is calculated to make the corresponding metathesis pathway (**4M*σ* → 4Mm**) exothermic by 6.7 kcal mol^{-1} compared to an endothermicity of 3.3 kcal mol^{-1} for **3M*σ* → 3Mm**. Changing the ligand from Cl^- in **2a** to OSO_3H^- in **4a** increases the exothermicity by 6.4 kcal mol^{-1}. No barrier appeared in linear transit studies between **4M*σ′*** and **4Mm**, and the hydroxy-oxygen-bound isomer (**4Mm′**) of **4Mm** proved less stable than **4Mm** by 12.1 kcal mol^{-1}. Both data support the notion that transfer of the activated hydrogen to a peripheral oxygen on the OSO_3H^- ligand is the favored pathway.

Also shown in Figures 1 and 3 (in parentheses) are the relative energies in the gas phase. As above, removal of solvation effects causes a general trend of stabilization for all species. For $n = 3$, 4 with OSO_3H^- as the ancillary ligand, metathesis is even more preferred over oxidative addition in the gas phase than in solution.

Conclusions

The calculations reported in this study address some of the points raised in the Introduction. Including the bidentate bipyrimidine ligand explicitly affects the results in two ways. One, the bidentate nature of the ligand means that nitrogen ligand dissociation processes of the type observed by Hush et al.[7] do not appear along the reaction coordinate and thus that the system must find other ways for the methane molecule to attack the platinum center. We note in this regard that we explored briefly the potential surface for axial attack of methane on (bipyrimidine)$PtCl_2$ and found this to be of far higher energy demand than the reaction steps described above.

Two, the presence of the peripheral nitrogen atoms allows for their protonation. Our calculations indicate that protonation increases the likelihood that the mechanism involves the metathesis pathway. However,

estimates suggest that protonation without additional coordination of counterions to the platinum is rather endothermic, so it appears that of the four molecules examined in this study, **1a** and **3a** are the more likely candidates for the Catalytica catalyst. Since modeling the sulfuric acid solvent is difficult, this theory remains tentative.

To the extent it holds, one then should consider the energetics of the substitution reactions of the experimental starting material (bipyrimidine)$PtCl_2$ which provide **1a** and **3a**. Unfortunately, our current solvation model is not accurate enough to estimate the heat of reaction for the substitution process:

$$\text{(bipyrimidine)}PtCl_2 + 2H_2SO_4 \rightarrow \text{(bipyrimidine)}PtOSO_3H^+ + HSO_4^- + 2HCl \quad (5)$$

However, our calculations suggest that the active species is **1a** if the equilibrium lies to the left. In that case C−H activation takes place by oxidative addition and the barrier is determined by the energy required for methane to replace one of the Cl anions in (bipyrimidine)$PtCl_2$. If the equilibrium lies to the right, the active species is **3a**, and C−H activation occurs by σ-bond metathesis. In that case the barrier is the activation energy for the process **3cy** → **3M*σ***. We estimate an upper bound for this barrier to be 38.9 kcal mol^{-1}. We suspect that the need to run the reaction at 180−220 °C stems from the fact that methane has to displace the coordination of either one Cl^- ligand or one HSO_4^- oxygen.

Acknowledgment. We thank Drs. Mary Chan, Liqun Deng, and Cory Pye of the Ziegler research group, and Dr. Roy Periana of Catalytica and the University of Southern California for helpful discussions. Funding of this work was provided by NSERC, the Canada Council (Killam Fellowship to T.Z.), and Northern Illinois University (Sabbatical leave to T.M.G.).

Supporting Information Available: Selected optimized structural parameters of the molecules examined in this study. This material is available free of charge via the Internet at http://pubs.acs.org.

OM0007264